Vertically Curved Girder Flanges

R. SHANKAR NAIR

Flange plates in steel girders are sometimes bent or curved in the vertical plane to accommodate changes in girder depth. For example, this detail occurs frequently in continuous-span bridge girders that are haunched to provide additional depth at the interior supports, as indicated in Fig. 1. The bottom flange of the girder in Fig. 1 is curved in the vertical plane at each transition between the horizontal and sloping configuration. Curves in flange plates are also common in steel pier bents and other kinds of bridge and heavy building construction (a few examples are sketched in Fig. 11).

Most designers recognize that a bend or out-of-plane curve in a flange plate, in conjunction with longitudinal tension or compression in the plate, will give rise to out-of-plane (nominally vertical) forces in the flange that will, in turn, produce transverse flexural stresses in the plate. Rigorous three-dimensional elastic analysis of the cylindrically curved plate is much too complicated to be attempted in most real design-office situations. Consequently, transverse flexure of the plate and the possible reduction in effectiveness of the flange are seldom considered in any rational manner, even in the design of very large structures.

Simple procedures for evaluating the effectiveness or efficiency of vertically curved flange plates will be developed in this paper. Conditions in the elastic range and at ultimate will be studied separately.

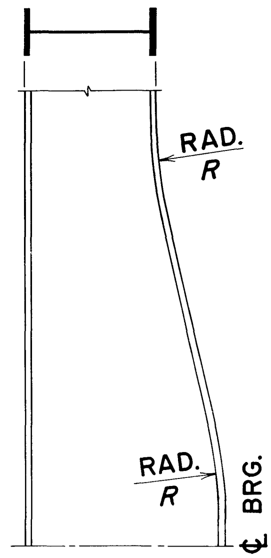

Fig. 1. Example of vertical curves in girder flange

ELASTIC ANALYSIS

Idealized Flange Behavior—The basic simplifying assumption in the elastic analysis is that longitudinal stress due to tension or compression in the curved flange plate is constant across the entire width of the plate. Thus, it is assumed the distribution of longitudinal stress in the curved flange is the same as in a flat flange plate.

In reality, there will always be some transverse out-of-plane flexural deformation of the curved flange plate, which will result in partial relief of longitudinal stress in portions of the flange distant from the web (or webs) and a corresponding increase in stress near the web (or webs). This redistribution of longitudinal stress over the width of the flange will result in a reduction in the transverse flexural stresses. The simplifying assumption in this elastic analysis will, therefore, yield an upper-bound value of transverse flexural stress.

Transverse Flexural Stresses—Consider a flange plate of thickness t bent to a radius R. Let the longitudinal stress in the plate be f_a. The longitudinal force on a longitudinal strip of the plate of unit width will be tf_a. Shown in Fig. 2, maintenance of equilibrium along the curve requires a radial

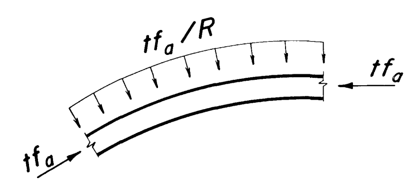

Fig. 2. Forces of longitudinal strip of flange of unit width

R. Shankar Nair is Vice President and Chief Structural Engineer, Alfred Benesch & Co., Consulting Engineers, Chicago, Illinois.

restraining force of tf_a/R per unit length of the longitudinal strip. This restraining force is provided by the transverse flexural stiffness of the plate. The effective out-of-plane (radial) loading on a transverse strip of flange plate in an

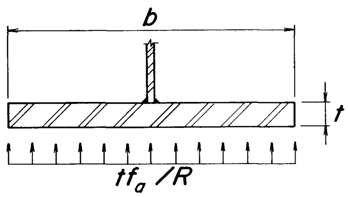

Fig. 3. Forces on transverse strip of flange of unit width

I-section girder is shown in Fig. 3. The maximum moment in a transverse strip of unit width is given by:

$$M = \frac{tb^2}{8R} f_a \qquad (1)$$

where b is the width of the flange plate. (For convenience, the reaction at the web is assumed to be concentrated at the center of the flange.) The section modulus of the strip is $t^2/6$ and the transverse flexural stress f_{bt} is given by:

$$f_{bt} = \frac{3b^2}{4Rt} f_a \qquad (2)$$

Equations 1 and 2 are also applicable to the flange of a box girder with dimensions defined in Fig. 4. In this case, the webs are taken as line supports along the edges of the flange.

As an example to illustrate the importance of transverse flexure, consider a 1.5-in. thick by 30-in. wide-flange plate bent to a radius of 360 in. This flange size and bend radius are not unusual in highway bridge girders. Applying Eq. 2, the transverse flexural stress in this flange is found to be 1.25 times the longitudinal stress.

Flange Efficiency Based on First Yield—For simplicity, the Tresca yield criterion (described elsewhere in this paper) will be used in this analysis. If transverse and longitudinal stresses are related to each other as indicated by Eq. 2, the Tresca criterion will indicate that yield will occur when the following condition is satisfied:

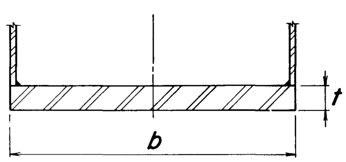

Fig. 4. Box girder flange

$$\left(1 + \frac{3b^2}{4Rt}\right) f_a = F_y \qquad (3)$$

The flange efficiency at start of yielding e_y is defined as the ratio of the longitudinal force at start of yielding in the curved flange plate to the longitudinal force at start of yielding in a flat flange plate of the same width and thickness. From Eq. 3, the following is obtained:

$$1/e_y = \left(1 + \frac{3b^2}{4Rt}\right) \qquad (4)$$

For the example considered earlier (b = 30, t = 1.5, R = 360), Eq. 4 would indicate an efficiency of 0.444.

The flange efficiency indicated by Eq. 4 corresponds to the start of local yielding at the center of the width of the flange at one surface of the plate (the surface at which longitudinal and transverse stresses are of opposite sign). These conditions do not necessarily represent failure or the limit of serviceability of the flange, as discussed in the next section.

PLASTIC ANALYSIS

Yield Criterion—This study of conditions at ultimate in curved-flange plates will be based on the Tresca straight-line yield criterion, shown graphically in Fig. 5. (For comparison, the more accurate von Mises criterion is also shown.) In the figure, f_1 and f_2 represent principal stresses perpendicular to each other. If f_1 and f_2 are of the same sign, yield occurs when either of the stresses is equal to F_y, regardless of the value of the other stress. If f_1 and f_2 are of opposite

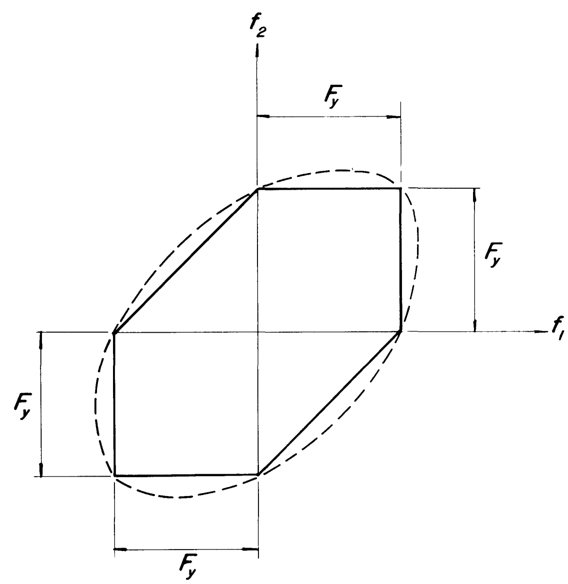

Fig. 5. Tresca yield criterion (solid lines) and von Mises yield criterion (broken lines)

signs, yield occurs when the sum of the absolute values of f_1 and f_2 is equal to F_y.

Stresses at Ultimate in Plate Element—Consider a plate element of thickness t and unit width and length, subject to direct force p in one direction (defined as the longitudinal direction) and movement M in the other direction (transverse). The transverse and longitudinal stresses produced by the maximum possible combination of transverse moment M and longitudinal force p (consistent with the Tresca yield criterion and fully plastic behavior) is shown in Fig. 6. The factor k can vary between 0 and ½, depending on the ratio of M to p. The limit on the value of M is given by:

$$M \leq \frac{1}{4} F_y t^2 \tag{5}$$

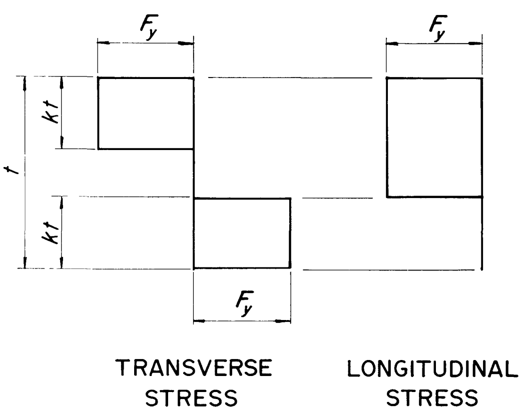

Fig. 6. Stresses in plate element at ultimate

From the stress distributions indicated in Fig. 6, it can be shown that for any value of M, the maximum possible value of p is as follows:

$$p = \left[\frac{1}{2} + \frac{1}{2}\left(1 - \frac{4M}{F_y t^2}\right)^{1/2}\right] F_y t \tag{6}$$

Stresses at Ultimate in Flange Plate—In plastic analysis, any assumed distribution of internal forces and stresses that satisfies equilibrium at all locations (without exceeding plastic stress limits at any location) will correspond to a load capacity less than or equal to the true plastic load limit. It is appropriate, therefore, to choose a stress distribution that results in the highest possible ultimate capacity, subject to equilibrium conditions and plastic stress limits. The following analysis is consistent with this approach.

In a curved-flange plate in a fully plastic state at ultimate, the transverse moment and longitudinal stress can be taken to be related to each other as indicated by Eq. 6 *at every location across the width of the flange*. This condition, together with equilibrium requirements at all locations, will establish the stress distribution corresponding to the greatest possible total longitudinal force in the flange. (As explained later, an exception has to be made for certain flanges in which Eq. 6 and equilibrium conditions cannot be satisfied simultaneously throughout the width of the flange.)

Schematic cross-sectional representations of I-section and box-section flange plates of width b and thickness t are shown in Fig. 7. Web reactions are considered to be con-

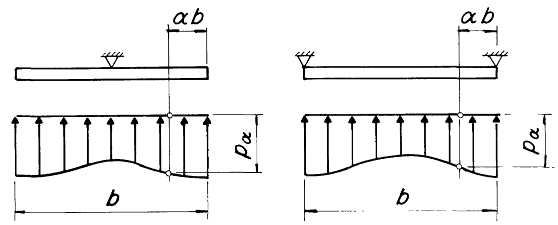

Fig. 7. Idealized I-section and box-section flanges and definition of longitudinal force

centrated at the center of the I-section flange and along the edges of the box girder flange. The distribution of longitudinal force in the flange is also shown schematically in Fig. 7. The longitudinal force per unit width at distance αb from the edge of the flange is denoted as p_α. The flange plate and all forces are symmetric about the center of the flange.

If the flange plate is bent to a radius R, longitudinal force p_α will generate a radial ("vertical") force of p_α/R on the flange. From statics, the resulting transverse moment, M_x, at any distance xb from the edge of the flange (with $x \leq ½$) is as follows:

$$\text{I-section: } M_x = \frac{b^2}{R}\int_0^x \int p_\alpha \, d\alpha \, d\alpha \tag{7a}$$

Box-section: M_x =

$$\frac{b^2}{R}\left\{x\int_0^{1/2} p_\alpha \, d\alpha - \int_0^x \int p_\alpha \, d\alpha \, d\alpha\right\} \tag{7b}$$

Equations 7a and b are the basic equilibrium conditions for the flange plate. These equilibrium conditions, together with Eq. 6 (which defines "ultimate" condition), establish the stresses in the flange at ultimate.

Flange Efficiency at Ultimate—The total longitudinal force in the flange at ultimate, P_u, is given by:

$$P_u = b \int_0^1 p_\alpha \, d\alpha \tag{8}$$

and the flange efficiency at ultimate, e_u, can be expressed as follows:

$$e_u = \frac{P_u}{F_y bt} = \frac{1}{F_y t}\int_0^1 p_\alpha \, d\alpha \qquad (9)$$

Solution of Equations—The equilibrium equation (Eq. 7) and the equation that defines the ultimate state (Eq. 6) constitute a non-linear system of equations that can be solved numerically for any particular combination of values of the variables. The method of solution is explained in greater detail in Appendix A.

By manipulation of the form of Eqs. 6, 7 and 9, it can be shown (see Appendix A) that flange efficiency at ultimate, e_u, depends only on the value of the single combined dimensionless variable b^2/Rt. The yield stress, F_y, does not affect e_u. The individual geometric variables, b, t, and R, affect e_u only to the extent that they are represented in the term b^2/Rt.

Numerical Evaluation and Exceptions to Ultimate Criterion—Since the flange efficiency at ultimate depends only on a single variable (b^2/Rt), it is possible to evaluate numerically the efficiency for many different values of the variable. The relationship between e_u and b^2/Rt has been determined numerically in this way. The procedure used is described in Appendix A.

The numerical analysis showed that if b^2/Rt is greater than 2.11 for an I-section flange or 3.03 for a box-section flange, Eqs. 5, 6 and 7 cannot be satisfied simultaneously at all locations across the width of the flange. Equation 7 represents equilibrium conditions and Eq. 5 represents an absolute limit on moment; these conditions cannot be violated. It follows, therefore, that if b^2/Rt is beyond the limits indicated, there must be some deviation from Eq. 6 in at least a part of the flange, with p being lower than indicated by Eq. 6. The deviation from Eq. 6 that results in the highest total longitudinal force in the flange, while allowing Eqs. 5 and 7 to be satisfied, occurs when p conforms to Eq. 6 within a distance of $0.5\sqrt{2.11\,Rt}$ from the web of an I-section flange or $0.5\sqrt{3.03\,Rt}$ from the webs of a box-section flange; p = 0 at greater distance from the web(s). Figure 8 shows the distribution of longitudinal force and transverse moment in an I-section flange at ultimate with b^2/Rt equal to 1.2, 2.11 and 4.0. Figure 9 shows similar data for a box-section flange with b^2/Rt equal to 1.2, 3.03 and 6.0.

Flange efficiencies at ultimate for I-section and box-section flanges for a wide range of values of b^2/Rt are presented in Table 1. For comparison, flange efficiencies at start of yielding (computed using Eq. 4) are also included in the tabulation. The data in Table 1 is presented graphically in Fig. 10.

In the example considered earlier (b = 30, t = 1.5, R = 360), flange efficiency at start of yield was found to be 0.444. From Table 1 or Fig. 10, it may be determined that the same plate has an efficiency at ultimate of about 0.91 as an I-section flange or 0.86 as a box-girder flange.

From the numerically determined data summarized in Table 1, simple equations relating e_u and b^2/Rt have been developed. Equations 10a and 10b, below, represent the tabulated data with an accuracy of better than 1%. Equation 10c is an exact representation of the data. In the following, the quantity b^2/Rt is denoted by the symbol β.

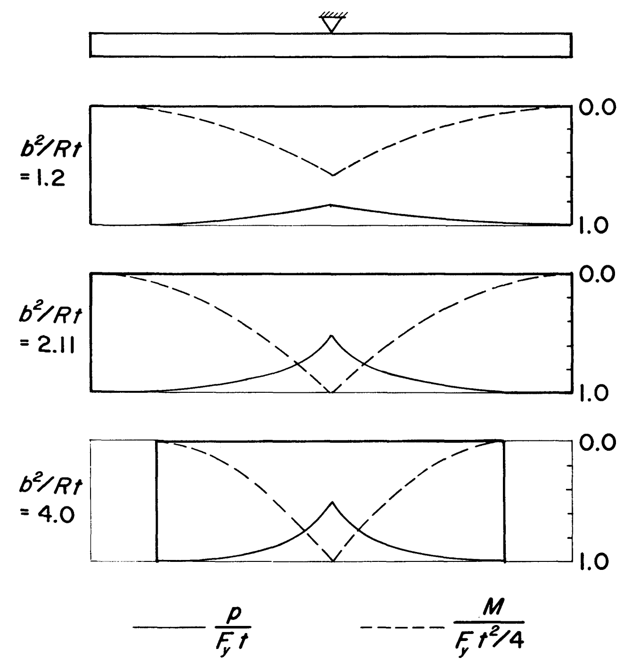

Fig. 8. Longitudinal force and transverse moment at ultimate in I-section flange with b^2/Rt = 1.2, 2.11 and 4.0

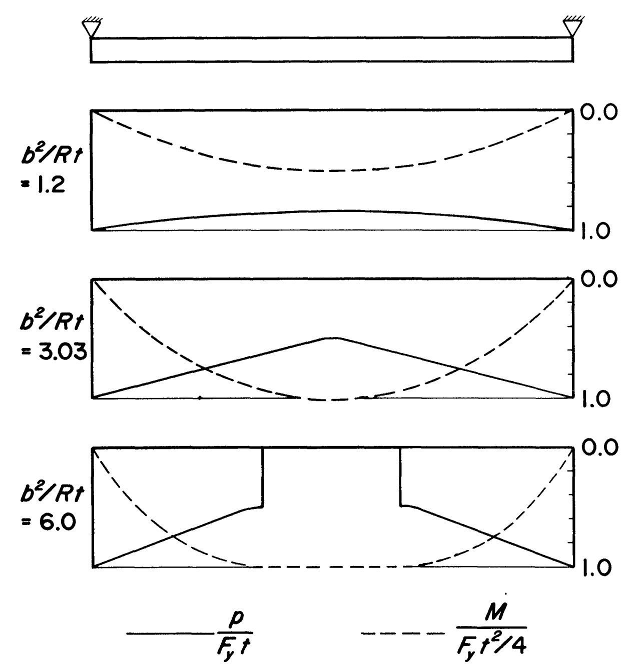

Fig. 9. Longitudinal force and transverse moment at ultimate in box-section flange with b^2/Rt = 1.2, 3.03 and 6.0

Table 1. Flange Efficiency

$\frac{b^2}{Rt}$	Efficiency at ultimate, e_u I-section	Efficiency at ultimate, e_u Box-section	Efficiency at start of yield, e_y
0.0	1.000	1.000	1.000
0.4	0.983	0.967	0.769
0.8	0.965	0.933	0.625
1.2	0.945	0.900	0.526
1.6	0.924	0.866	0.455
2.0	0.898	0.833	0.400
2.11[a]	0.889	—	—
2.4	0.834	0.798	0.357
2.8	0.772	0.763	0.323
3.03[b]	—	0.741	—
4	0.645	0.645	0.250
6	0.527	0.527	0.182
8	0.456	0.456	0.143
10	0.408	0.408	0.118
20	0.288	0.288	0.063
40	0.204	0.204	0.032

[a] Limit of full flange width effectiveness for I-section flange
[b] Limit of full flange width effectiveness for box-section flange

I-section flange with $\beta < 2.11$:

$$e_u = 1 - 0.052\,\beta \tag{10a}$$

Box-section flange with $\beta < 3.03$:

$$e_u = 1 - 0.085\,\beta \tag{10b}$$

I-section flange with $\beta \geq 2.11$ and box-section flange with $\beta \geq 3.03$:

$$e_u = 1.29/\sqrt{\beta} \tag{10c}$$

The equation for efficiency at start of yield (Eq. 4) can be rewritten in terms of β as follows:

$$e_y = 1/(1 + 0.75\,\beta) \tag{11}$$

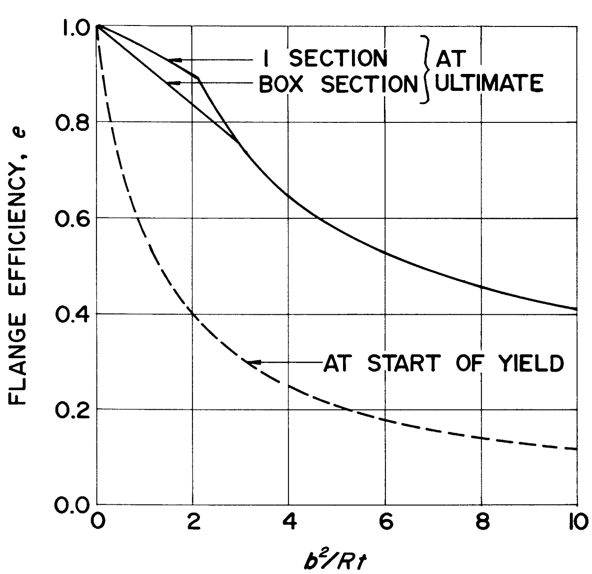

Fig. 10. Relationships between flange efficiency and b^2/Rt

DISCUSSION OF RESULTS AND SUGGESTIONS FOR DESIGN

The elastic analysis of vertically curved flange plates has shown that the plate curvature can cause very significant transverse flexural stresses, and major reductions in the longitudinal force that the flange can resist without yielding. The transverse stresses and the reduction in longitudinal capacity (based on first yield) are large, even in flanges with commonly used dimensions and radii of curvature.

The results of the plastic analysis provide an unusually vivid demonstration of the additional capacity available in many structures as a result of plastic behavior after the start of local yielding. Table 1, and Fig. 10, show the dramatic difference between flange capacity at start of yielding and the ultimate capacity based on plastic behavior. In the specific example mentioned ($b = 30$, $t = 1.5$, $R = 360$), the curvature caused a 56% reduction in flange load at start of yield but only a 9% or 14% reduction (depending on configuration, I or box) in capacity at ultimate.

The concept of taking advantage of post-yield capacity in the design of steel structures is well established. Current design criteria for hybrid girders are an obvious example of the use of this concept in the bridge field. The start of yielding in a curved flange plate is a very local phenomenon, occurring near the middle of the width of the flange, at one surface of the plate. The curved flange is, therefore, especially well suited to a design procedure that takes advantage of post-yield behavior.

The results of this study indicate the reduction in flange capacity caused by curvature should not be ignored during design. The reduction in capacity should be checked; if it is found to be small it could be neglected, but the decision to neglect the effect of curvature should always be a deliberate decision that is made after assessing the magnitude of the effect.

It is suggested that the flange efficiency at ultimate be used for design regardless of whether the overall design of the structure is by working stress or ultimate load techniques. The flange efficiency, e_u, can be computed very easily from Eq. 10 or obtained graphically from Fig. 10. The *effective* cross-sectional area of the flange should then be taken as e_u times the actual area. This reduced area should be used in all moment and stress computations to account for the reduction in flange capacity caused by curvature.

Fatigue effects and the possibility of local buckling of the flange should be considered, as appropriate. The radial force or reaction exerted by the curved flange against the web might also be significant in some cases. The magnitude of this radial force on the web (or on two webs, if a box-section), per unit length of flange, is equal to the total longitudinal force in the flange divided by the radius of curvature. The web and the web-flange connection should be checked for this force.

The analysis and discussion in this paper has specifically dealt with vertically curved flanges in I-section and box-section girders. The analysis and the resulting equations are also applicable to cylindrically curved plates in a wide range of other structures. A few examples of curved plates (other than vertically curved girder flanges) to which this study is applicable are sketched in Fig. 11.

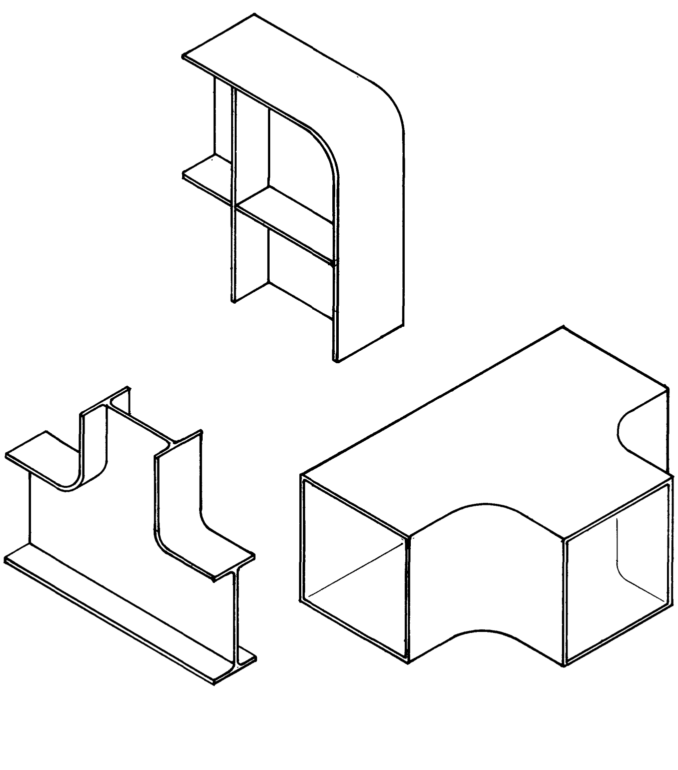

Fig. 11. Examples of curved plates other than vertically curved girder flanges

SUMMARY AND CONCLUSIONS

Vertically curved flange plates in I-section and box-section girders have been analyzed. Separate elastic and plastic analyses have been performed. These analyses have resulted in the development of simple equations and charts for determining the reduction in flange capacity caused by the curvature.

It has been found that the curvature can cause very large transverse flexural stresses and very large reductions in the load at which yielding of the flange begins, even in flanges with commonly used dimensions and radii of curvature. It was also found, however, that through plastic behavior, the flange can resist considerable additional load after the start of yielding. The curvature causes a much smaller reduction in *ultimate* flange capacity than in the load at which yielding begins.

The results of this study indicate the reduction in flange capacity caused by vertical curvature should be taken into account in design. Simple procedures and equations for this purpose have been suggested.

NOMENCLATURE

b = Width of flange plate

e_u = Flange efficiency at ultimate (longitudinal force at ultimate divided by $F_y bt$)

e_y = Flange efficiency at start of yield (longitudinal force at start of yield divided by $F_y bt$)

F_y = Yield strength of steel in flange

f_1 = Principal stress on plate element, perpendicular to f_2

f_2 = Principal stress on plate element, perpendicular to f_1

f_a = Average longitudinal direct stress in flange (elastic analysis only)

f_{bt} = Transverse flexural stress at center of flange (elastic analysis only)

k = A factor that defines depth of flexural stress block at ultimate

M = Transverse moment per unit width of plate; if subscripted, subscript denotes location

P_u = Longitudinal force in flange at ultimate

p = Longitudinal force per unit width of plate; if subscripted, subscript denotes location

R = Radius of curvature of plate

t = Thickness of plate

x = Distance from edge of plate, expressed as a ratio of b

α = Distance from edge of plate, expressed as a ratio of b

β = b^2/Rt

γ = $p/F_y t$; if subscripted, subscript denotes location

δ = $M/F_y t^2$; if subscripted, subscript denotes location

APPENDIX A. SOLUTION OF EQUATIONS

The non-linear system of equations that defines the problem can be simplified by introducing new dimensionless variables, γ and δ, as follows:

$$\gamma = \frac{p}{F_y t} \tag{A1}$$

$$\delta = \frac{M}{F_y t^2} \tag{A2}$$

Equations 5 and 6 can now be rewritten as:

$$\delta \leq \frac{1}{4} \tag{A3}$$

$$\gamma = \frac{1}{2} + \frac{1}{2}(1 - 4\delta)^{1/2} \tag{A4}$$

Equation 7 takes the following form (with $x \leq 1/2$):

$$\text{I-section: } \delta_x = \frac{b^2}{Rt}\int_0^x \int \gamma_\alpha \, d\alpha \, d\alpha \tag{A5a}$$

Box-section: $\delta_x =$

$$\frac{b^2}{Rt}\left\{ x \int_0^{1/2} \delta_\alpha \, d\alpha - \int_0^x \int \delta_\alpha \, d\alpha \, d\alpha \right\} \tag{A5b}$$

The equation for flange efficiency, Eq. 9, can be rewritten as:

$$e_u = \int_0^1 \delta_x dx \tag{A6}$$

It is clear from Eq. A3 through A6 that the flange efficiency at ultimate, e_u, is a function only of the quantity b^2/Rt. For any given value of b^2/Rt, the value of e_u can be determined from Eqs. A4, A5 and A6 through the use of any of various available techniques for numerical integration and numerical solution of non-linear equation systems. The method that was used in the present study is outlined below.

Method of Numerical Solution—Because of the symmetry of the flange, it was only necessary to work with one half of the width of the flange. The half width of the flange was divided into 100 equal segments, thus creating 101 equally spaced nodes between the edge of the flange and the center. These nodes represent 101 values of α and x, increasing in steps of 0.005 from 0 at the edge to 0.5 at the center. An iterative method of solution was adopted, as follows:

Step 1a: Assume value of γ at all nodes.

Step 1b: Compute δ at all nodes, based on γ from Step 1a, using Eq. A5.

Step 2a: Compute new values of γ at all nodes, based on δ from Step 1b, using Eq. A4.

Step 2b: Compute new values of δ at all nodes, based on γ from Step 2a, using Eq. A5.

Continue until convergence. Then compute e_u, using Eq. A6.

To achieve convergence for the box-section flange at high values of b^2/Rt, an adjustment had to be made in the iteration procedure. In every step after the first, the computation of δ was based not on the most recent set of γ values, but on the average of the two most recent sets of γ.

For the I-section flange, γ in Step 1 was taken as unity at all nodes. For the box-section flange, more rapid convergence was achieved (especially for values of b^2/Rt greater than about 1.6) by assuming γ in Step 1 to be varying uniformly from 1.0 at $x = 0$ to 0.5 at $x = 0.5$.

If Eq. A3 is violated at any node, Eq. A4 would involve a square root of a negative quantity. If this occurs at any stage in the iteration, the analysis would break down even if the violation of Eq. A3 is only a temporary occurrence in the iterative procedure, which will not occur in the final converged solution. To avoid this problem, if δ was greater than $1/4$ at any location in any intermediate step of the solution procedure, the sign of the term $(1 - 4\delta)$ in Eq. A4 was reversed before applying the square root and reversed again after the square root. If δ remained greater than $1/4$ at any node in the final converged solution, it was concluded that Eq. A3 through A5 could not be solved simultaneously for the particular value of b^2/Rt that was being tried.